Bioorganic & Medicinal Chemistry Letters xxx (2017) xxx–xxx

Contents lists available at ScienceDirect

Bioorganic & Medicinal Chemistry Letters

journal homepage: www.elsevier.com/locate/bmcl

Discovery of AAT-008, a novel, potent, and selective prostaglandin EP4 receptor antagonist

Yoshiyuki Okumura [a,*,1], Tatsuya Yamagishi [b,1], Seiji Nukui [c], Kazunari Nakao [d]

[a] AskAt Inc., 4F Ito Bldg., 4-11-28 Meieki Nakamura-ku, Nagoya 450-0002, Japan
[b] Discovery Research, RaQualia Pharma Inc, 8F Daiwa Meieki Bldg., 1-21-19 Meieki Minami, Nakamura-ku, Nagoya 450-0003, Japan
[c] INC Research, 16F Shinagawa East One Tower, 2-16-1 Konan, Minato-ku, Tokyo 108-0075, Japan
[d] Discovery Research, Mochida Pharmaceutical Co., Ltd., 722 Uenohara, Jimba, Gotemba, Shizuoka 412-8524, Japan

ARTICLE INFO

Article history:
Received 3 October 2016
Revised 17 January 2017
Accepted 24 January 2017
Available online xxxx

Keywords:
EP4 receptor antagonist
Structure–activity relationship (SAR)
Prostaglandin E2
Inflammation
Pain
Autoimmune diseases
Cancer
Clinical candidate

ABSTRACT

Starting from acylsufonamide HTS hit **2**, a novel series of *para*-*N*-acylaminomethylbenzoic acids was identified and developed as selective prostaglandin EP4 receptor antagonists. Structural modifications on lead compound **4a** were explored with the aim of improving potency, physicochemical properties, and animal PK predictive of QD (once a day) dosing regimen in human. These efforts led to the discovery of the clinical candidate AAT-008 (**4j**), which exhibited significantly improved pharmacological profiles over grapiprant (**1**).

Prostaglandin E_2 (PGE_2) is a pro-inflammatory mediator generated from arachidonic acid by the action of cyclooxygenase (COX) isoenzymes under inflammatory conditions. Four PGE_2 receptor subtypes (EP1, EP2, EP3, and EP4) responsible for different pharmacological properties have been cloned and classified.[1,2] The EP4 subtype, a G-protein-coupled receptor (GPCR), stimulates cyclic adenosine monophosphate (cAMP) production[3] and is distributed in a wide variety of tissues suggesting an important role of EP4 receptor in PGE_2-mediated biological events such as inflammation,[4] pain,[5] and cancer.[6–10] Selective blockade of the PGE_2 signaling through the EP4 receptor pathway represents an attractive approach to discover novel analgesic, immunomodulating, and antineoplastic agents. Analgesic potentials are clearly supported by the reduction of pain and inflammation in EP4 receptor knock out/knock down animals and the similar results using EP4 receptor selective antagonists in animal studies.[11,12] Since the PGE_2-EP4 signal blockade does not affect actions of the other subtype PGE_2 receptors as well as other prostanoids, selective EP4 antagonists might provide analgesic effects without adverse events observed with nonsteroidal anti-inflammatory drugs (NSAIDs) or cyclooxygenase-2 (COX-2) inhibitors,[13–15] and are expected to be a new therapy for the treatment of both acute and chronic inflammatory pain. In addition, selective EP4 receptor antagonists are also expected to offer an attractive therapeutic approach for autoimmune diseases such as inflammatory bowel disease (IBD), rheumatoid arthritis (RA), and multiple sclerosis (MS)[16–18] through the inhibition of interleukin-23 (IL-23) production and suppression of T helper 1 (Th1) and T helper 17 (Th17). Moreover, the recent reports suggest that the EP4 receptor which is expressed in certain types of cancer promotes tumor cell proliferation and metastasis.[19] Therefore, selective antagonism of the EP4 receptor might have significant clinical potential for the treatment of colorectal, breast, prostate, lung, gastric, bladder, head and neck, hepatocellular, pancreatic, and ovarian cancers. Herein we report novel and selective EP4 receptor antagonists of benzoic acid with the nicotinamide or benzamide scaffolds.

Grapiprant (Fig. 1) is a selective antagonist for prostaglandin E_2 (PGE_2) receptor subtype 4 (EP4) identified as a clinical candidate for the treatment of inflammatory pain associated with osteoarthritis (OA). It is currently under development for use in humans[20] and dogs.[21] The projected dosing regimen of grapiprant

* Corresponding author.
E-mail address: yoshiyuki.okumura@askat.co.jp (Y. Okumura).
[1] These authors contributed equally to this work.

http://dx.doi.org/10.1016/j.bmcl.2017.01.067
0960-894X/

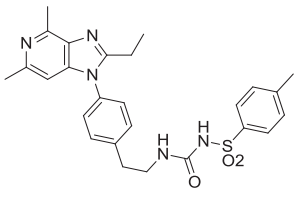

Fig. 1. Selective EP4 antagonist, grapiprant under development.

for humans is 50–100 mg, PO, BID (twice a day) based on the pharmacology and pharmacokinetic (PK) data in clinical studies.

In order to identify another clinical candidate with improved efficacy, safety, and pharmacokinetic profiles with potential for QD (once a day) dosing, we embarked on a back-up discovery project to discover the second generation of grapiprant (**1**).[22] The target profiles of this candidate are summarized as follows. The back-up candidate should demonstrate improved potency over grapiprant, i.e.; (1) antagonize PGE_2-mediated cAMP elevation in transfectants expressing human EP4 receptor-with a $pA_2 > 8.6$; (2) exhibit selectivity of >100 over other PG receptor subtypes; (3) clearly demonstrate improved oral activity over grapiprant in key acute and chronic inflammatory pain models; i.e., carrageenan induced mechanical hyperalgesia and complete Freund's adjuvant (CFA) induced weight bearing deficit in the rat; (4) demonstrate a PK profile in animals predictive of QD dosing in human. From a medicinal chemistry perspective, the back-up compound should have improved physicochemical characteristics; lower molecular weight and lower lipophilicity while improving efficacy and PK profile. In order to meet the above criteria, we pursued an alternative core structure different from the sulfonylurea since the structure–activity relationships (SAR) studies around grapiprant revealed compounds consisting of the sulfonylurea core had extremely low volume of distribution and high to moderate clearance in rats and other experimental animals.

High throughput screening (HTS) of the Pfizer compound library using a human EP4 functional assay measuring PGE_2-induced cAMP formation in HEK-293 cells expressing human EP4 receptor and the subsequent verification in a membrane binding assay using [^{3}H]PGE_2 resulted in the identification of *N*-acyl sulfonamide **2** as a moderately potent EP4 antagonist (IC_{50}: 302 nM) without EP4 selectivity over other subtypes (Fig. 2). HTS hit **2** has high molecular weight (MW: 610.08) and is quite lipophilic (ALogP: 5.70, cLogD: 5.80).[23] Further screening of HTS hit **2** were initiated by using the in-house compound libraries. First, a bioisosteric transformation[24,25] of the *N*-acyl phenylsulfonamide moiety to the corresponding carboxy group was well tolerated and resulted in the identification of compound **3** with reduced molecular weight. Compound **3** displayed modest EP4 selective functional antagonism (IC_{50}: 370 nM) and good stability in human liver microsomes (HLM) ($T_{1/2} > 120$ min), however it did not have acceptable physicochemical properties (typically for lead compounds, solubility in phosphate-buffered saline (PBS) > 10 μM; molecular weight <400; ALogP < 4) (Fig. 2). Next, with further reduction of MW and lipophilicity (ALogP and cLogD) in mind, a structural similarity search by using a simplified pharmacophore query as shown in Fig. 2 led to identify ca. 1000 compounds. The subsequent filtering of these compounds by applying Lipinski's rule of 5[26,27] and eliminating compounds with toxicophore[28–30] narrowed down to 50 hit compounds. These 50 compounds were evaluated in a series of assays of functional EP4 receptor antagonism, binding selectivity against EP receptors, HLM stability, human cytochrome P450 inhibition, aqueous solubility, and membrane permeability. As a result, compound **4a** was shown to be superior to the others, demonstrating EP4 selective functional antagonism (IC_{50}: 575 nM), binding affinity for EP4 receptor (*Ki*: 73 nM), stability in HLM ($T_{1/2} > 120$ min), no notable CYP 450 inhibition, high Caco-2 cell permeability (P_{app}: 25×10^{-6} cm/s),[31] good solubility in PBS (>10 μM), lower MW (MW: 384.33), and acceptable lipophilicity (ALogP: 3.61, cLogD: 2.14). The hit-to-lead efforts resulted in the identification of compound **4a** that has a core structure of *para*-*N*-acylaminomethylbenzoic acid (Fig. 2). The molecules containing carboxylic acid often have undesirable metabolic instability, limited permeability, and potential toxicities. Despite the drawbacks of the carboxylic acid functional group, **4a** exhibited selective EP4 functional antagonism with a suitable metabolic profile *in vitro* and good physicochemical properties. Thus, we envisaged that the optimization efforts around **4a** would provide the backup candidate that meets the target profiles.

The optimization of the lead compound (**4a**) was initiated and the initial key SAR and the results of the structural modifications of lead compound **4a** are summarized in Fig. 3. Replacement of the carboxylic acid moiety with other functional groups led to loss of functional activity against EP4 receptor. Although the corresponding tetrazole exhibited slightly increased functional activity, the tetrazole analog was a substrate for efflux pumps and a strong inhibitor of CYP3A4. Shifting the carboxylic acid moiety from *para*- to *meta*-position showed loss of intrinsic activity. The benzoic acid moiety was not replaceable by nicotinic acid, cyclohexanecarboxylic acid, or 4-thiazolecarboxylic acid. Moreover, modifications of the amide moiety by exchanging the nitrogen with methylene, reduction of the amide carbonyl, or *N*-methylation of the nitrogen

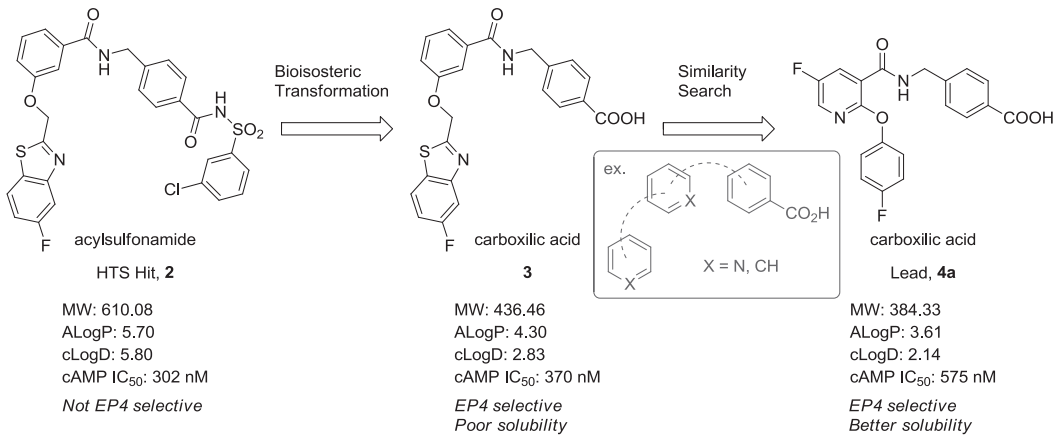

Fig. 2. Hit to lead: genesis of benzoic acid EP4 antagonists.

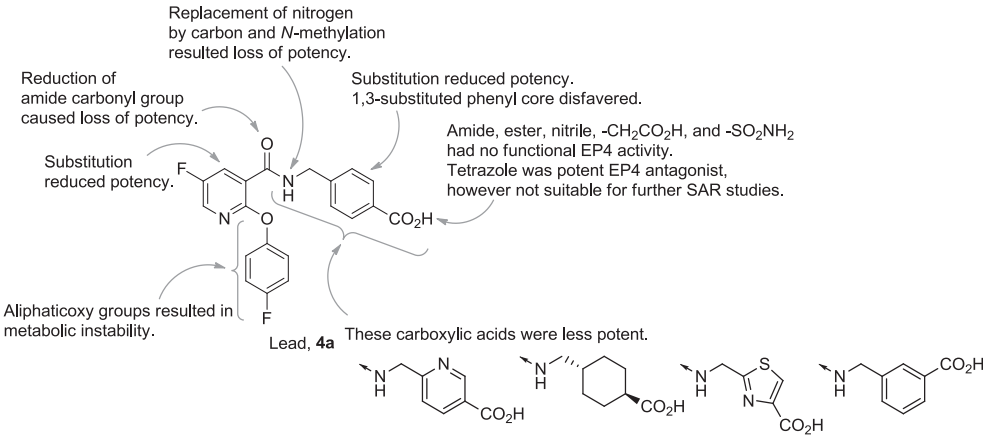

Fig. 3. Lead optimization: initial SAR study results.

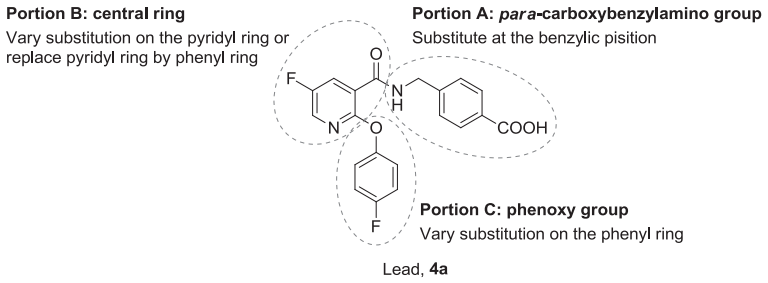

Fig. 4. Lead development: completion of optimization strategy for lead compound **4a**.

also reduced intrinsic activity. These early SAR studies of the *para*-(aminomethyl)benzoic acid moiety of lead compound **4a** showed that the carboxylic acid group at the *para*-position was a key element for the EP4 antagonist activity. A limited class of substituents on the phenoxypyridine moiety of lead compound **4a**, maintained or enhanced the potencies when satisfied regiochemical requirements. The introduction of a substituent to the 4-position of pyridine ring caused loss of intrinsic activity. Additionally, it was found that the aliphaticoxy groups were not suitable surrogates for the phenoxy group on the 2-position of the pyridine of **4a**. Even though the aliphaticoxy substituted analogs retained intrinsic activity, their metabolic stabilities in HLM were decreased.

In order to develop detailed SAR around lead compound **4a** for improving its profile, structural modifications were performed in three portions of lead compound **4a**: the benzylic position of *para*-aminomethylbenzoic acid moiety for Portion A, the central ring core with substituents for Portion B, and the substitution pattern of the phenoxy group for Portion C (Fig. 4). Furthermore, this strategy allowed us to easily construct the molecule in a concerted manner for effective SAR studies.[32] We aimed to improve not only pharmacological properties, but also physiochemical properties such as MW < 450 and cLogD < 3,[33] although the compounds with a MW over 450 and a cLogD over 3 were prepared for exploring SAR involving the selective EP4 antagonist.

Our optimization studies on lead compound **4a** started by exploring portions A and B. The synthetic route to the target compounds from easily available materials is outlined in Scheme 1. Starting from *ortho*-halo-substituted aromatic acids **5** or **6**, the corresponding methyl esters were formed, which were then converted to *ortho*-phenoxy-substituted aromatic acids **7** or **8** with nucleophilic aromatic substitution (SNAr) reaction followed by alkali hydrolysis. Depending on the aromatic ring (A = CH or N) of starting materials **5** or **6**, the phenol was reacted under different conditions. The SNAr reaction of the benzoates derived from benzoic acids **6** (A = CH) required more severe reaction conditions than that of the nicotinates derived from nicotinic acids **5** (A = N). The target benzoic acids **4** and **11** were prepared by reaction of carboxylic acids **7** or **8** with *para*-(methoxycarbonyl)benzylamine using EDCI/HOBt condensation conditions and subsequent hydrolysis of the methyl ester or *t*-butyl ester intermediates **9** or **10** thereby obtained.

The human EP4 binding and functional activities of representative compounds are presented in Table 1. Switching the aromatic ring in portion B from pyridine to benzene was tolerated (**4a** vs **11a**). Replacement of 5-fluoro substituent on the pyridine ring moiety of lead compound **4a** with 5-chloro substituent showed about 2-fold increase in EP4 binding and functional activity (**4a** vs **4b**). The 5-chlorobenzene analogs were almost equipotent to the corresponding 5-chloropyridine analogs (**4b** vs **11b**) although it is concerned that benzene **11b** has an evidently high cLogD value by 0.6 units relative to pyridine **4b** (3.21 vs 2.60). Substitution of hydrophilic functionality such as carboxamides, sulfones and sulfonamides on the benzene ring was also attempted, however none of them exhibited sufficient EP4 antagonistic activity at all (data not shown). 5-Methylpyridine and 6-methylpyridine analogs (**4c** and **4d**) displayed substantially decreased EP4 functional activity. Incorporation of a methyl group at the benzylic position in portion A led to a marked improvement in EP4 binding and functional activity in a stereochemical dependent manner (**4e**, **4f**, and **11c**). The (*S*)-methyl isomers were dramatically more active than the corresponding antipodes (**4f** vs **4g**). The geminal methyl groups or ethyl group at the same position decreased the binding affinity (**4h** and **4i**). Key compounds exhibiting EP4 antagonist activities were selected and tested to assess selectivity against the other EP receptor subtypes. These compounds did not show any significant binding to EP1 and EP3 at the highest concentration tested

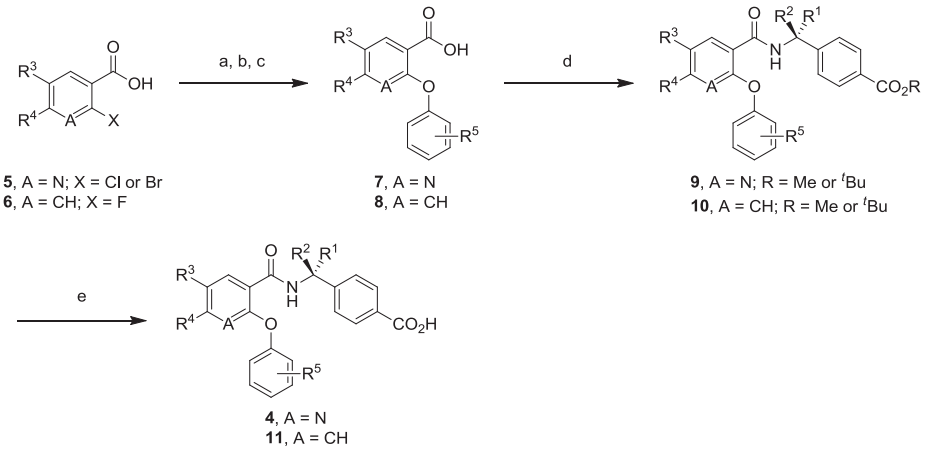

Scheme 1. R^1, R^2, R^3, R^4, and R^5 fragments are given in Tables 1 and 2; Reagents and conditions: (a) H_2SO_4, MeOH reflux, 58–99%; (b) NaH, "phenol", DMF, 120 °C, 65–87% or K_2CO_3, "phenol", toluene, reflux, 77–99% or Cu, CuI, K_2CO_3, "phenol", DMF, reflux, 68–92%; (c) NaOH-H_2O, MeOH, r.t., 80–99%; (d) EDCI, HOBt, "benzylamine", Et_3N, CH_2Cl_2, r.t., 73–93%; (e) NaOH-H_2O, MeOH, r.t., 60–91% or TFA, CH_2Cl_2, r.t., 79–93%.

Table 1
Optimization around portion A & B of *para*-*N*-acylaminomethylbenzoic acid.

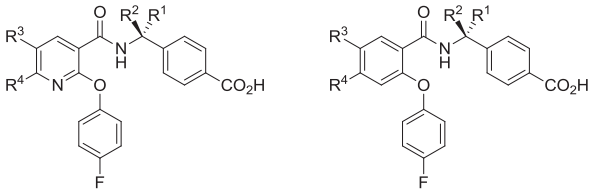

Compd	R^1, R^2	R^3	R^4	MW	cLogD	hEP4 functional cAMP IC_{50} (nM)	Binding IC_{50} (nM)				Caco-2[a] A-B P_{app} ($\times 10^{-6}$ cm s^{-1})
							hEP4	hEP1	hEP2	hEP3	
4a	H, H	F	H	384.33	2.14	575	104	>20,000	>20,000	>20,000	25.3
11a	H, H	F	H	383.35	2.75	317	124	>20,000	236	>20,000	36.3
4b	H, H	Cl	H	400.79	2.60	254	37.9	>20,000	1290	>20,000	20.1
11b	H, H	Cl	H	399.80	3.21	101	21.6	N.D.	N.D.	N.D.	51.4
4c	H, H	Me	H	380.37	2.42	2940	N.D.	N.D.	N.D.	N.D.	N.D.
4d	H, H	H	Me	380.37	2.21	>5000	N.D.	N.D.	N.D.	N.D.	N.D.
4e	(S)-Me	F	H	398.36	2.54	143	28.7	N.D.	N.D.	N.D.	30.2
4f	(S)-Me	Cl	H	414.81	2.99	25.9	9.68	>20,000	4360	>20,000	30.3
11c	(S)-Me	Cl	H	413.83	3.61	38.2	6.59	>20,000	709	>20,000	32.4
4g	(R)-Me	Cl	H	414.81	2.99	1210	N.D.	N.D.	N.D.	N.D.	25.3
4h	Me, Me	F	H	412.39	3.07	N.D.	545	N.D.	N.D.	N.D.	36.3
4i	*rac*-Et	F	H	412.39	3.21	N.D.	181	N.D.	N.D.	N.D.	20.1

N.D. = Not determined.
[a] *In vitro* permeability (Papp, apical to basolateral) at pH 6.5/7.4 determined in Caco-2 cells.

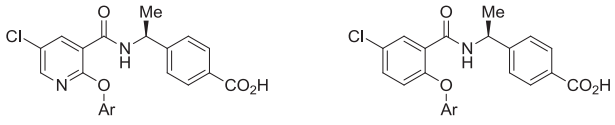

Fig. 5. Scaffolds of EP4 antagonist.

(20 μM). Although some compounds were found to have weak binding affinity to EP2, most of compounds (**4f** and **11c**) showed high selectivity to EP4, including compounds with candidate credentials. In the Caco-2 assay, compound **4f** and **11c** exhibited sufficiently high permeability.

Based upon these findings on portions A and B, novel scaffolds of EP4 antagonist, **12** and **13** (R^1 & R^2 = (*S*)-Me; R^3 = Cl; R^4 = H), shown in Fig. 5, were identified. We next focused on optimizing portion C of these scaffolds.

We utilized Scheme 2 for an alternative synthesis of nicotinamide scaffold **12**, which is quite effective for derivatization of portion C. Thus nicotinic acid **14** was coupled with *tert*-butyl 4-[(1*S*)-1-aminoethyl]benzoate using EDCI/HOBt condition to give 2-chloro-nicotinamide **15**. Nucleophilic displacement of 2-chloro-nicotinamide **15** with appropriately substituted phenols afforded 2-phenoxy-nicotinamides **9**. A final acid hydrolysis of *tert*-butyl ester moiety in intermediates **9** under acidic conditions furnished respective benzoic acids **4**.

A SAR of the representative analogs of portion C are shown in Table 2. Substitution at the *meta*-position of the benzene ring in portion C of nicotinamide scaffold (**12**) with a fluorine or chlorine atom enhanced the functional activity as compared with the corresponding *ortho*- or *para*-positions (**4j** vs **4k** or **4f**, **4l** vs **4m** or **4n**). Therefore, the *meta*-substitution was explored in more details. The introduction of small and electron-withdrawing substituents such as fluoro, chloro, cyano, and trifluoromethyl at the *meta*-position of the benzene ring was found favorable (**4j**, **4l**, **4o**, and **4p**). Among

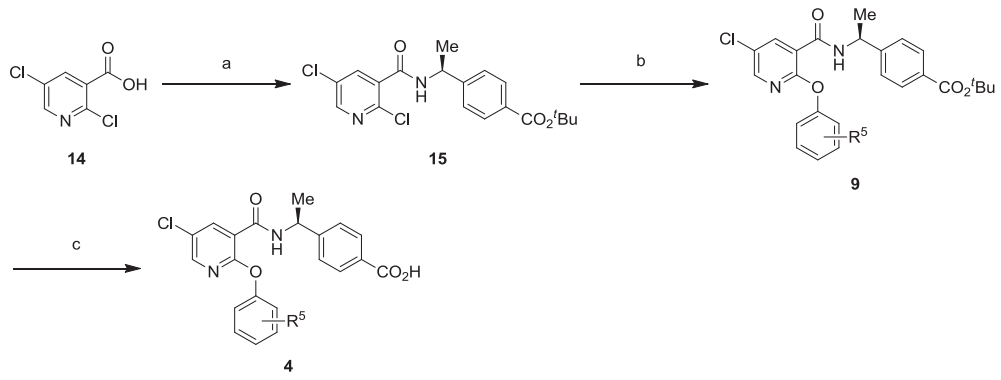

Scheme 2. R^5 given in Table 2; Reagents and conditions: (a) EDCI, HOBt, "benzylamine", Et_3N, CH_2Cl_2, r.t., 70%; (b) BEMP, "phenol", toluene, 110 °C, 72–93%;[34] (c) TFA, CH_2Cl_2, r.t., 61–86%

Table 2
Optimization around portion C of *para*-*N*-acylaminomethylbenzoic acid.

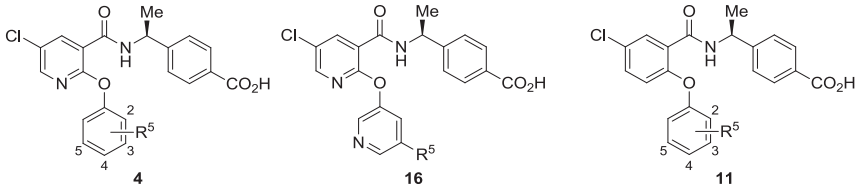

Compd	R^5	MW	cLogD	hEP4 functional cAMP IC_{50} (nM)	Binding IC_{50} (nM)				Caco-2[a] A-B P_{app} ($\times 10^{-6}$ cm s^{-1})
					hEP4	hEP1	hEP2	hEP3	
4j	3-F	414.81	2.99	16.3	2.40	>20,000	1890	>20,000	20.1
4k	2-F	414.81	2.99	61.4	N.D.	N.D.	N.D.	N.D.	N.D.
4f	4-F	414.81	2.99	25.9	9.68	>20,000	4360	>20,000	30.3
4l	3-Cl	431.27	3.45	21.8	5.02	N.D.	N.D.	N.D.	N.D.
4m	2-Cl	431.27	3.45	93.5	N.D.	N.D.	N.D.	N.D.	N.D.
4n	4-Cl	431.27	3.45	94.3	N.D.	N.D.	N.D.	N.D.	N.D.
4o	3-CN	421.83	2.67	36.2	13.4	>20,000	3320	>20,000	N.D.
4p	3-CF_3	464.82	3.73	60.4	N.D.	N.D.	N.D.	N.D.	N.D.
4q	3-OMe	426.85	2.77	340	N.D.	N.D.	N.D.	N.D.	N.D.
4r	3-SMe	442.92	3.33	400	N.D.	N.D.	N.D.	N.D.	N.D.
4s	3-OCF_3	480.82	4.91	1790	N.D.	N.D.	N.D.	N.D.	N.D.
16a[b]	F	415.80	1.84	175	N.D.	N.D.	N.D.	N.D.	N.D.
16b[b]	Cl	432.26	2.30	137	N.D.	N.D.	N.D.	N.D.	N.D.
11d	3-F	413.83	3.61	30.6	8.76	>20,000	1620	>20,000	41.9
11e	3-Cl	430.28	4.06	41.1	N.D.	N.D.	N.D.	N.D.	N.D.
11c	4-F	413.83	3.61	38.2	6.59	>20,000	709	>20,000	32.4

N.D. = Not determined.
[a] *In vitro* permeability (Papp, apical to basolateral) at pH 6.5/7.4 determined in Caco-2 cells.
[b] This compound was prepared according to the reaction sequence shown in Scheme 1 by using "5-substituted-3-hydroxypyridine" instead of "phenol".

the four analogs, *meta*-fluoro analog **4j** was the most active compound. Although di-fluoro substituted analogs such as 3,4-di-fluoro-, 2,3-di-fluoro-, 2,5-di-fluoro-, and 3,5-di-fluoro-analog exhibited IC_{50} values of less than 50 nM in the functional assay (data not shown), these analogs did not surpass the functional activity of **4j**. On the other hand, the substitution with electron-donating groups such as methoxy or methylthio at the *meta*-position appeared to be less favorable (**4q** and **4r**). Trifluoromethoxy group at the *meta*-position was not tolerated at all (**4s**). Replacement of the phenyl group in portion C by 3-pyridyl group decreased the functional activity (**16a** and **16b**). Incorporation of hydrophilic functionality such as carboxamides, sulfones, and sulfonamides on the benzene ring also caused substantial decrease in intrinsic activity (data not shown). A similar tendency in the SAR studies of the analogs with benzamide scaffold (**13**) were observed, however approximately 2-fold less potent than the corresponding nicotinamide scaffold analogs (**4j** vs **11d**, **4l** vs **11e**) with the exception of **11c**, which displayed equivalent *in vitro* activity to **4f**. Key compounds (**4j**, **4o**, and **11d**) that exhibited potent EP4 functional activity were evaluated for their selectivity against the other EP receptor subtypes. These potential compounds showed sufficient EP4 selectivity. Furthermore, compounds **4j**, **4o**, and **11d** had high permeability in the Caco-2 assay.

Based on these SAR studies, six compounds which exhibit IC_{50} values <40 nM in the human EP4 functional assay were selected for further characterization. Table 3 shows comparative data of the six compounds. All the compounds showed high metabolic stability in HLM ($T_{1/2}$ > 120 min). Although the intrinsic activity of 3-cyano analog **4o** was sufficient to progress to the next stage, **4o** was found to be positive in the *in vitro* micronucleus test[35] and suffered from poor membrane permeability and high efflux ratio in the Caco-2 assay at equivalent pH condition (P_{app} A to B: 0.644×10^{-6} cm/s, P_{app} B to A: 25.8×10^{-6} cm/s, Efflux Ratio: 40).[36] It was found that the 3-chloro analog **4l** was not a pure

Table 3
Comparative profiles of potential six compounds.

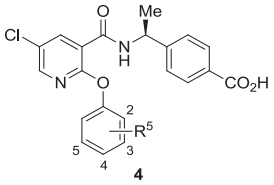

4

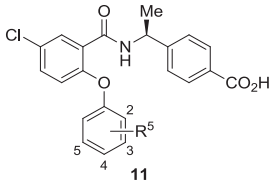

11

Compd	R^5	hEP4 functional cAMP IC_{50} (nM)	hEP4 binding IC_{50} (nM)	HLM $T_{1/2}$ (min)	hEP4 functional cAMP pA_2	CIMH[a] MED (mg/kg)
4f	4-F	25.9	9.68	>120	8.61	10
4j (AAT-008)	3-F	16.3	2.40	>120	8.97	1
4l	3-Cl	21.8	5.02	>120	N.D.	N.D.
4o	3-CN	36.2	13.4	>120	N.D.	N.D.
11c	4-F	38.2	6.59	>120	8.75	10
11d	3-F	30.6	8.76	>120	8.90	10

N.D. = Not determined.
[a] CIMH = carrageenan induced mechanical hyperalgesia.

Table 4
Comparative *in vitro* profiles of AAT-008 (**4j**) and grapiprant (**1**).

Assay	AAT-008 (4j)	Grapiprant (1)
In vitro binding to prostaglandin receptors		
Recombinant human EP1: K_i[a] (nM)	>6000	>5000
Recombinant human EP2: K_i[a] (nM)	1836	>5000
Recombinant human EP3: K_i[a] (nM)	>6000	>5000
Recombinant human EP4: K_i[b] (nM)	0.97 ± 0.09	13 ± 4
Recombinant human DP: K_i[a] (nM)	>6000	2926
Recombinant human FP: K_i[a] (nM)	>6000	>5000
Recombinant human IP: K_i[a] (nM)	>6000	>5000
Human TP (platelet): K_i[b] (nM)	>6000	>5000
Recombinant rat EP4: K_i[c] (nM)	6.1 ± 0.3	20 ± 1
Recombinant dog EP4: K_i[c] (nM)	38 ± 1	24 ± 3
In vitro inhibition of functional activity		
PGE_2-induced cAMP in human EP4 transfectant: pA_2[c]	8.97 ± 0.06	8.32 ± 0.03
PGE_2-induced cAMP in rat EP4 transfectant: pA_2[c]	8.34 ± 0.05	8.19 ± 0.16[d]
PGE_2-induced cAMP in mouse EP4 transfectant: pA_2[b]	9.00	8.11

[a] N = 2.
[b] N = 1.
[c] Values are the Mean ± SE (N = 3).
[d] N = 4.

antagonist but a partial agonist, therefore it is assumed that the functional antagonism of **4l** (IC_{50}: 21.8 nM) was caused by its partial agonism. The remaining four compounds (**4f**, **4j**, **11c**, and **11d**) were subsequently re-evaluated for their *in vitro* antagonistic potencies (pA_2 values) against human EP4 receptor and oral activity in the rat carrageenan induced mechanical hyperalgesia model. Among them, **4j** showed the highest potency which met the backup candidate criteria (pA_2: 8.97), and was selected for preclinical development with code AAT-008.

As shown in Table 4, AAT-008 (**4j**) selectively antagonized the prostaglandin receptor EP4. AAT-008 inhibited [^{3}H]-PGE_2 binding to human EP4 receptor with a K_i value of 0.97 nM and had more than 1000-fold selectivity over other prostaglandin receptors, such as EP1, EP2, EP3, DP, FP, IP, and TP. AAT-008 showed potent binding affinity for human, rat, and dog EP4 receptors, with K_i values of 0.97, 6.1, and 38 nM, respectively. In the human EP4 receptor highly expressed in HEK293 cells, AAT-008 significantly suppressed PGE_2-induced elevation of intracellular cAMP level in a PGE_2-competitive fashion with a pA_2 value of 8.97 (1.1 nM). Compared with grapiprant (**1**), AAT-008 was approximately 4-fold more potent in the functional assay.

The *in vitro* ADME profile of AAT-008 (**4j**) was very promising, with high stability in HLM. The pre-clinical pharmacokinetic properties of AAT-008 were also assessed in rats (Sprague-Dawley, male), dogs (beagle, male), and monkeys (cynomolgus, male). The experimentally determined parameters are summarized in Table 5. AAT-008 was absorbed into the systemic circulation following oral administration to rats, dogs, and monkeys with a T_{max} of 0.438–8.00 h. In all the pre-clinical species, AAT-008 showed good oral bioavailability in rats, dogs, and monkeys with 73.6%, 80.6%, and 73.3%, respectively. AAT-008 had a pharmacokinetic profile with low clearance (CL_{total}) and moderate volume of distribution (Vd_{ss}). After intravenous injection of AAT-008 at the dose of 1 mg/kg, the plasma elimination half-life ($T_{1/2}$) values are 4.59 h in rats, 8.43 h in dogs, and 14.5 h in monkeys.

Moreover, AAT-008 (**4j**) had a significantly improved pharmacological profile over grapiprant, as was demonstrated in acute and chronic inflammatory pain models in rats (Table 6). The oral dosing of AAT-008 reduced carrageenan induced mechanical hyperalgesia in rats in a dose dependent manner with an MED 1 mg/kg, PO at 1-h post dosing (vs 30 mg/kg, PO for grapiprant). In a model of chronic inflammatory pain, CFA induced weight bearing deficit in the rat, AAT-008 exhibited an analgesic effect in a dose dependent

Table 5
IV and PO pharmacokinetics of AAT-008 (**4j**).[a]

Species	Route	C_{max} (ng/mL)	T_{max} (h)	$AUC_{0\text{-inf}}$ (ng h/mL)	$T_{1/2}$ (h)	CL_{total} (mL/min/kg)	Vd_{ss} (L/kg)	*F*%
Rat	IV	–	–	9620 ± 1180	4.59 ± 1.05	1.75 ± 0.24	0.593 ± 0.104	–
	PO	994 ± 244	0.750 ± 0.289	7090 ± 3330	3.71 ± 0.39	–	–	73.6 ± 34.5
Dog	IV	–	–	7490 ± 1510	8.43 ± 2.47	2.30 ± 0.50	1.21 ± 0.33	–
	PO	1450 ± 320	0.438 ± 0.125	6080 ± 1590	7.95 ± 2.88	–	–	80.6 ± 10.6
Monkey	IV	–	–	3390 ± 1120	14.5 ± 5.1	5.31 ± 1.60	4.70 ± 0.87	–
	PO	76.0 ± 17.2	8.00 ± 0.00	2460 ± 879	21.9 ± 8.1	–	–	73.3 ± 14.1

Values are the Mean ± SD (N = 4).
[a] Compound was administered at a dose of 1 mg/kg (rats, dogs, and monkeys) intravenously (IV) or orally (PO).

Please cite this article in press as: Okumura Y., et al. Bioorg. Med. Chem. Lett. (2017), http://dx.doi.org/10.1016/j.bmcl.2017.01.067

Table 6
Comparative *in vivo* profiles of AAT-008 (**4j**) and grapiprant (**1**).

Assay	AAT-008 (4j)	Grapiprant (1)
In vivo effects: acute and chronic inflammatory pain		
Carrageenan-induced mechanical hyperalgesia in rats: MED (mg/kg, PO)	1 (n = 3)	30 (n = 2)
CFA-induced weight bearing deficit in rats: MED (mg/kg, PO)	1 (n = 3)	20 (n = 2)

manner with an MED of 1 mg/kg, PO (vs 20 mg/kg, PO for grapiprant). AAT-008 exhibited good passive permeability and good metabolic stability in HLM ($T_{1/2}$ > 120 min) or hepatocytes ($T_{1/2}$ > 360 min). Inhibitory effects of AAT-008 (1 μM) on CYP1A, CYP2C9, CYP2C19, CYP2D6, and CYP3A activities were determined to be less than 5%.

In conclusion, a novel series of *para*-*N*-acylaminomethylbenzoic acid-based selective prostaglandin EP4 receptor antagonists has been identified, starting from *N*-acyl sulfonamide HTS hit **2**, followed by hit-to-lead optimization using in-house compound library. Lead compound **4a** was sequentially optimized by dividing it into three parts. The most significant improvement was achieved when a (*S*)-methyl substituent was introduced at the benzylic position. Eventually, **4j** (AAT-008) was identified as a development candidate, having excellent potency, selectivity for EP4, and metabolic stability. Superior potency of AAT-008 to grapiprant was demonstrated in different *in vivo* models. AAT-008 was stable in human liver microsomes or hepatocytes and was predicted to be well absorbed in humans. AAT-008 was selected as a candidate for preclinical development and subsequent clinical studies.[20] The projected efficacious oral dosing regimen of AAT-008 for OA pain is 1–20 mg QD.

Acknowledgements

The authors would like to acknowledge EP4 receptor antagonist project teams at PGRD, Nagoya.

A. Supplementary material

Supplementary data associated with this article can be found, in the online version, at http://dx.doi.org/10.1016/j.bmcl.2017.01.067.

References

1. Narumiya S, Sugimoto Y, Ushikubi F. *Physiol Rev*. 1999;79:1193.
2. Kawahara K, Hohjoh H, Inazumi T, Tsuchiya S, Sugimoto Y. *Biochim Biophys Acta*. 2015;1851:414.
3. Ichikawa A, Sugimoto Y, Negishi MJ. *Lipid Mediators Cell Signall*. 1996;14:83.
4. McCoy JM, Wicks JR, Audoly LP. *J Clin Invest*. 2002;110:651.
5. St.-Jacques B, Ma W. *Pain*. 2013;154:313.
6. Mutoh M, Watanabe K, Kitamura T, et al. *Cancer Res*. 2002;62:28.
7. Fujino H, Regan JW. *Trends Pharmacol Sci*. 2003;24:335.
8. Yang L, Huang Y, Porta R, et al. *Cancer Res*. 2006;66:9665.
9. Kundu N, Ma X, Kochel T, et al. *Breast Cancer Res Treat*. 2014;143:19.
10. Majumder M, Xin X, Liu L, Girish GV, Lala PK. *Cancer Sci*. 2014;105:1142.
11. Lin C-R, Amaya F, Barrett L, et al. *J Pharmacol Exp Ther*. 2006;319:1096.
12. Nakao K, Murase A, Ohshiro H, et al. *J Pharmacol Exp Ther*. 2007;322:686.
13. Hippisley-Cox J, Coupland C. *BMJ*. 2005;330:1366.
14. Hippisley-Cox J, Coupland C, Logan R. *BMJ*. 2005;331:1310.
15. Zimecki M. *Postepy Hig Med Dosw (Online)*. 2012;66:287.
16. Cua DJ, Sherlock J, Chen Y, et al. *Nature*. 2003;421:744.
17. Murphy CA, Langrish CL, Chen Y, et al. *J Exp Med*. 2003;198:1951.
18. Yen D, Cheung J, Scheerens H, et al. *J Clin Invest*. 2006;116:1310.
19. Yokoyama U, Iwatsubo K, Umemura M, Fujita T, Ishikawa Y. The prostanoid EP4 receptor and its signaling pathway. *Pharmacol Rev*. 2013;65:1010.
20. For more information, please see the AskAt Inc. <http://askat-inc.com/>.
21. For information on the development for dogs, please see the Aratana Therapeutics, Inc. <http://www.aratana.com/therapeutics/osteoarthritis-pain/>.
22. All authors were employed by Pfizer at the time this work was carried out. Intellectual properties regarding this work are all transferred to AskAt Inc.
23. ALogP (calculated partition coefficients, atom-based log*P*) and cLogD (calculated distribution coefficients at pH 7.4) were determined using Pipeline Pilot (http://accelrys.com/). The values of grapiprant (**1**) were calculated as follows: MW 491.61, ALogP 4.55, and cLogD 4.71.
24. Patani GA, LaVoie EJ. *Chem Rev*. 1996;96:3147.
25. Meanwell NA. *J Med Chem*. 2011;54:2529.
26. Lipinski CA, Lombardo F, Dominy BW, Feeney PJ. *Adv Drug Del Rev*. 1997;23:3.
27. Lipinski CA. *Drug Discovery Today*. 2004;1:337.
28. Smith GF. *Prog Med Chem*. 2011;50:1.
29. Williams DP, Naisbitt DJ. *Curr Opin Drug Discov Devel*. 2002;5:104.
30. Blagg J. Structural alerts for toxicity. In: Abraham DJ, Rotella DP, eds. *Burger's Medicinal Chemistry, Drug Discovery and Development*. 7th ed. NJ: John Wiley & Sons Inc.; 2010:301–334.
31. Human colon carcinoma cell line (Caco-2) permeability assay was performed at constant pH conditions (apical pH of 6.5 and basolateral pH of 7.4).
32. Compound synthesis and characterization and assay protocols have been published: Yamagishi T, Okumura Y, Nukui S, Nakao K. *PCT Int Appl*. 2005. WO2005021508.
33. Waring MJ. *Expert Opin Drug Discov*. 2010;5:235.
34. SNAr reaction using organic base is essential to afford the desired target products with better yield instead of using inorganic base to avoid producing byproducts, BEMP: 2-*tert*-Butylimino-2-diethylamino-1,3-dimethylperhydro-1,3,2-diazaphosphorine (CAS No.: 98015-45-3).
35. Matsuoka A, Yamazaki N, Suzuki T, Hayashi M, Sofuni T. *Mutat Res*. 1992;272:223.
36. Arturson P, Karlsson J. *Biochem Biophys Res Commun*. 1991;175:880.